SCIENCE FOR GLASS PRODUCTION

UDC 666.1.031.2:536.24

THE EFFECT OF FLAME LENGTH ON HYDRODYNAMICS OF GLASS-MELTING TANK IN A FURNACE WITH HORSESHOE-SHAPED FLAME

V. Ya. Dzyuzer[1] and V. S. Shvydkii[1]

Translated from Steklo i Keramika, No. 9, pp. 5 – 11, September, 2005.

It is demonstrated that the hydrodynamics of a melting tank of a contemporary highly efficient glass-melting furnace depends on a set of combined factors. Along with temperature distribution on the melt surface depending on exterior heat exchange, convection flows to a large extent depend on the tank design, the batch loading, and glass melt working conditions, as well as the working flow parameters determined by the specific output of the furnace. The combined analysis of the results of modeling external heat-exchange and the tank hydrodynamics suggest that the most advisable heating regime for the considered furnace design is when the total length of the flame is equal to the furnace length.

According to the method for constructing a mathematical model of a glass-melting furnace, the effect of exterior heat exchange parameters on hydrodynamics of the melting tank is manifested through the temperature field on the glass melt surface [1, 2]. The analysis of exterior heat exchange depending on the flame length [3] has yielded regression equations for calculating the temperature field on the glass melt surface and thus to specify the main boundary conditions for modeling.

Regression equations for calculation of temperature field on glass melt surface

$t(x, y)$, °C	l_{fl}/L_f
$t(x,y) = 1554.46 + 162.09x + 262.67y - 74.92x^2 - 1.03xy - 147.77y^2 + 0.06x^2y + 0.51xy^2 + 0.02x^2y^2 + 8.92x^3 + 23.64y^3 - 0.34x^4 - 1.29y^4$ . .	0.334
$t(x,y) = 1392.14 + 11.22x + 356.82y - 1.35x^2 - 7.98xy - 177.12y^2 + 0.86x^2y + 0.22xy^2 + 0.01x^2y^2 + 0.31x^3 + 28.24y^3 - 0.04x^4 - 1.50y^4$ . .	0.662
$t(x,y) = 1145.23 + 87.11x + 32.76y - 19.51x^2 - 1.24xy - 12.96y^2 + 0.13x^2y + 0.18xy^2 - 0.02x^2y^2 + 2.55x^3 + 1.95y^3 - 0.11x^4 - 0.10y^4$ . . .	1.000
$t(x,y) = 808.64 + 264.61x + 155.78y - 34.02x^2 - 28.36xy - 52.27y^2 + 2.30x^2y + 2.55xy^2 - 0.22x^2y^2 + 2.13x^3 + 6.64y^3 - 0.06x^4 - 0.30y^4$ . . .	1.216
$t(x,y) = 735.83 + 242.99x + 107.03y - 14.92x^2 - 36.48xy - 20.87y^2 + 2.87x^2y + 3.62xy^2 - 0.30x^2y^2 - 0.63x^3 + 0.98y^3 + 0.05x^4 + 0.02y^4$ . . .	1.430

The longitudinal section of the melting tank is shown in Fig. 1.

The tank dimensions are as follows (m): $AB = 9.2$; $BC = FG = 0.4$, $CD = 2.4$, $AH = 1.3$, $BF = CG = 0.8$, $HI = 4.0$, $DE = 0.3$, and the furnace length $AD = L_f = 13.62$. The installation of a spillway in the melting tank obviously complicates the analysis and at the same times brings the modeling conditions closer to the actual melting tank design in state-of-the-art glass-melting furnaces. The calculations are fulfilled for the furnace efficiency of 300 tons/day achieved under the specific glass melt output equal to 2.6 tons/(m^2 · day). Other source data are given in [1].

One of the most complicated and essentially little investigated problems in numerical modeling of glass-melting tank hydrodynamics is establishing boundary conditions regulating the arrival of newly formed melt at the tank and at the working zone. Specifying boundary conditions based on the working flow can be reduced to the mass flow rate determined by the furnace efficiency and the size of the tank neck and to specifying the site from which the melt goes to the

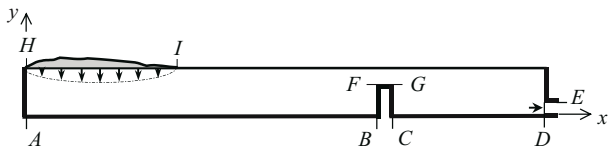

Fig. 1. Scheme of glass melt flow domain in the melting tank.

[1] Ural State Technical University (UPI), Ekaterinburg, Russia.

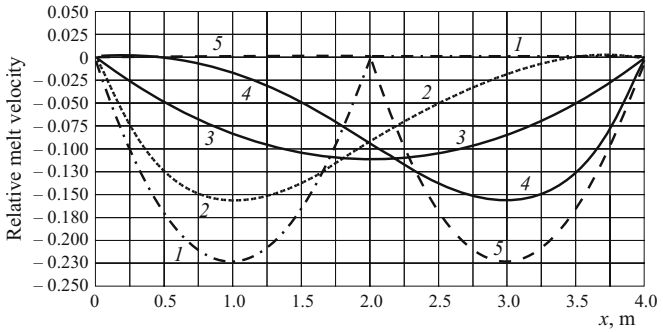

Fig. 2. Variants of velocity profiles of melt arriving at the tank. Surface area *S*: *1* – *5*) 0.2206, 0.2941, 0.4412, 0.5882, and 0.6618, respectively.

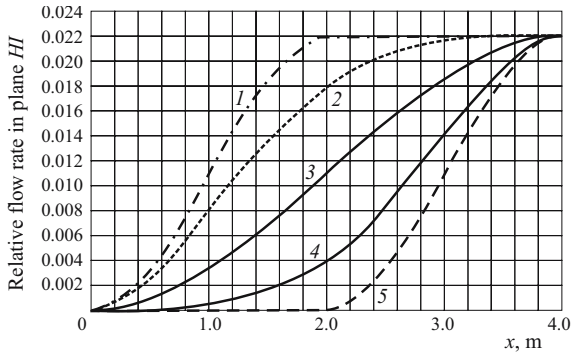

Fig. 3. Dynamics of melt arriving to the tank. Curve numbers correspond to velocity profile numbers in Fig. 2.

working zone: from the bottom of the tank via the section *DE* (Fig. 1). However for an equal flow rate the dynamics of the arriving flow may be different, since it depends on the batch melting conditions.

So far it has been difficult to formalize the physicochemical aspects of glass melting in the context of numerical modeling. Therefore, let us perform a certain simplification. Let us assume that the kinetics of the batch melting process can be expressed via the profile of the vertical velocity component at the batch – melt interface. Such profiles can be numerous. For quantitative analysis, let us consider the most typical ones. Figure 2 shows five variants of the velocity of melt arriving to the tank that ensure the melt inflow equal to its outflow. The represented velocity profiles characterize different dynamics of glass coming into the tank, which can be quantitatively estimated as the surface area *S* contained between the flow rate curve and the abscissa axis shown directly beside the curves (Fig. 3). A velocity profile variation in the plane *HI* modified the stream function and the flow vorticity boundary conditions. This, in turn, affects the regularities of convective heat exchange in the melting tank and the conditions of the formation of melt circulation contours. The profile accepted as the basic one in the present study has $S = 0.4412$, where the glass temperature calculation errors for different parts of the tank varies from + 1.4 to – 0.67%.

The results of modeling are represented by 2D fields of relative streamlines and glass melt temperatures (in all figures *x* and *y* are the longitudinal and the vertical coordinates of the melting tank, respectively). In Fig. 4 the streamlines are normalized over the glass mass flow rate through the section *DE* equal to 4.34 kg/sec. In constructing streamlines for the visible representation of calculation results, the scale was modified for certain sectors of the tank. The melt temperature distribution in Fig. 5 is represented in the form of normalized values of the isotherms (t_g/1000 [°C]).

Fuel combustion in a short flame ($l_{fl}/L_f = 0.334$) is characterized by highly heterogeneous temperatures not only on the glass melt surface (Fig. 6*a*, curve *1*), but also in the longitudinal section of the melting tank (Fig. 5*a*). The maximum value of the average temperature of the glass melt surface across the width of the working side of the furnace $\bar{t}_{g.\,s}$ equal to 1590°C is observed in the immediate vicinity of the left end wall of the tank (*AH*): $x \approx 0.7$ m. The difference of temperatures $\bar{t}_{g.\,s}$ on the segment $x \approx 0.70 - 13.62$ m is equal to 580°C and the temperature gradient is $\Delta\bar{t}_{g.\,s}/\Delta x = 44.9$ K/m. The temperature gradient toward the plane *AH* is not more than 5 K/m.

Let us consider the variation in the temperature difference across the tank depth (Fig. 6*b*, curve *1*). Approaching the spillway ($x \approx 8.8$ m), the surface temperature $\bar{t}_{g.\,s}$ and the bottom layer temperature $\bar{t}_{g.\,b}$ become leveled. At the same time, the condition $\bar{t}_{g.\,s} > \bar{t}_{g.\,b}$ is satisfied. Before the spillway and above it ($x \approx 8.8 - 9.6$ m) we observe a jumpwise increase in the temperature difference reaching approximately 220°C. Beyond the spillway ($x > 9.6$ m) the difference between the glass surface and bottom layer temperatures is characterized by the relation $\bar{t}_{g.\,s} < \bar{t}_{g.\,b}$ Immediately before the tank neck, the bottom layer temperature is about 275°C higher than that of the glass melt surface. At the same time, despite the low values of $\bar{t}_{g.\,s}$ (1220 – 1008°C), the mean glass melt temperature in the neck reaches 1285.5°C. The complicated temperature distribution in the longitudinal section of the melting tank (Fig. 5*a*) is obviously related to the mass exchange processes occurring in the melt.

The analysis of the distribution of the relative streamline function value (Fig. 4*a*) indicates that for the preset flame length l_{fl} several centers of convection melt flows are formed in the longitudinal section of the melting tank, whose origin cannot be attributed only to the thermal heterogeneity of the glass melt surface. The longitudinal coordinate of the first center of contour formation ($x \approx 0.7$ m) with a certain assumption corresponds to the location of $\bar{t}_{g.\,s}$. A circulation contour is formed to the right of the maximum, in which the medium circulates clockwise, whereas a smaller contour with counterclockwise circulation is formed on the left. The direction of surface flows coincides with the direction of the circulation contours, which can be arbitrarily associated to the charging and working glass melt convection cycles.

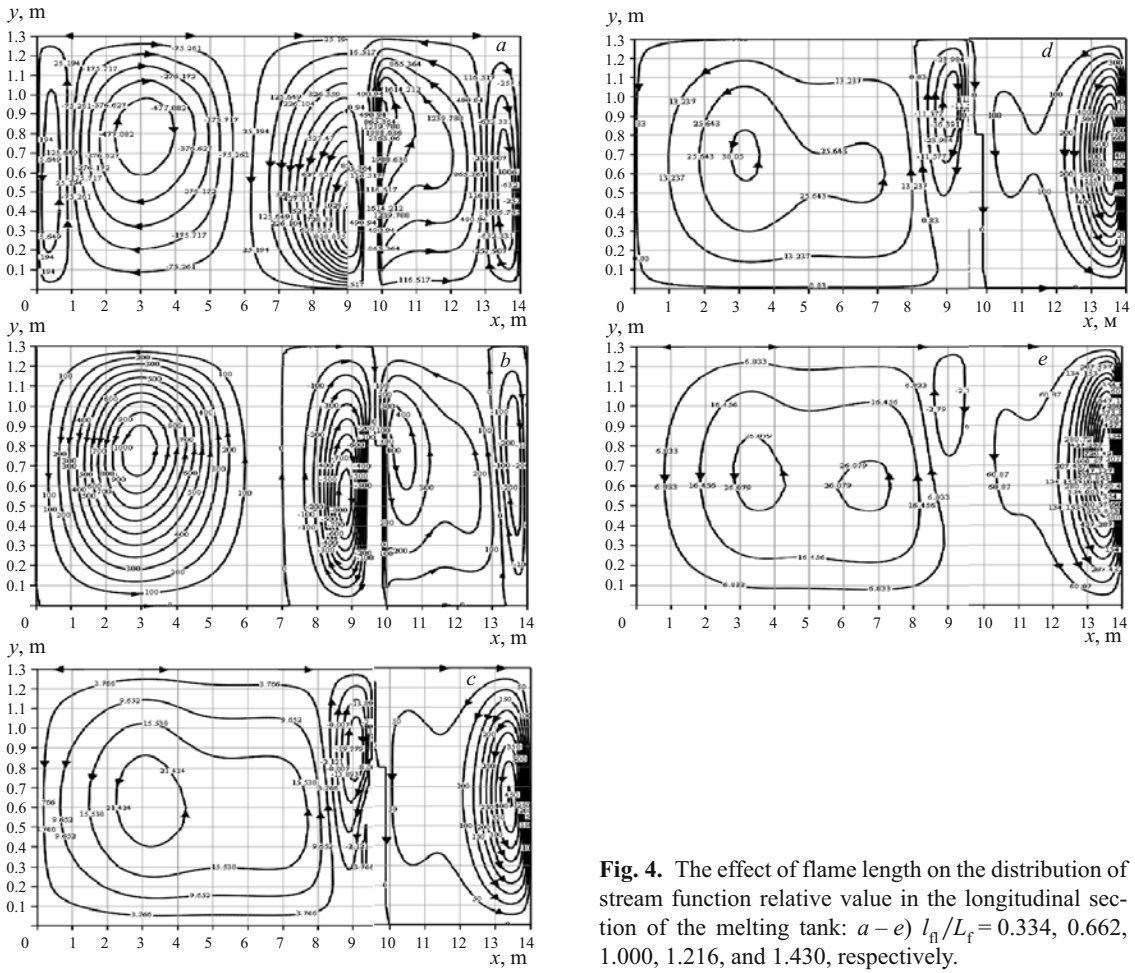

Fig. 4. The effect of flame length on the distribution of stream function relative value in the longitudinal section of the melting tank: *a* – *e*) $l_{fl}/L_f = 0.334$, 0.662, 1.000, 1.216, and 1.430, respectively.

The variation of $\bar{t}_{g.s}$ along the tank and temperature difference variation ($\bar{t}_{g.s} - \bar{t}_{g.b}$) suggest that the right-hand circulation contour should extend up to the spillway. However, the horizontal size of the contour is limited by the coordinate $x \approx 5.5$ m. At this particular distance from the left end wall we observe another plane dividing convection flows. As distinct from the contours with the coordinate $x \approx 0.7$ m, in this dividing plane we observe flows circulating toward each other. The origin of this contour and its circulation direction cannot be explained by the effect of the horizontal gradients of hydromechanical pressure and uplift force. Its formation to a large extent is presumably due to the conditions of melt arriving to the tank and the direction of the working glass melt flow.

At first glance, it seems appropriate to specify the right-hand boundary of the third circulation contour (starting from the plane *AH*) by the coordinate $x \approx 12.8$ m. In the given case the contour center in fact coincides with the spillway location, whereas the contour parameters in the vicinity of the spillway are modified without changing its circulation direction. At the same time, significant differences in glass melt circulation multiplicity before and after the spillway and the jump in temperature difference above the spillway horizontal plane *FG* give grounds to subdivide the third circulation contour into two independent convection cycles and thus to accept the left spillway plane *BF* as the right boundary of this contour. The limited possibilities of the graphic representation of streamlines (even using the method of modifying the image scale) prevent us from showing the full picture of the melt flow near the spillway. The counterclockwise circulation of the third contour implies the presence of an ascending melt flow moving along the plane *BF*. Upon flowing over the spillway, the glass melt becomes partly involved in the surface working flow. Part of the melt sinks along the plane *CG* and passes to the fourth circulation contour

Accepting the above concept of the formation of convection flows in the left part of the tank (before the spillway), note that the hydrodynamics of the melting zone is determined not only by the nonuniformity of temperature distribution on the melt surface and the presence of a tall spillway, but also by the dynamics of melt arriving at the tank and the working flow.

Let us consider the specifics of the formation of convection flows beyond the spillway. The circulation direction of the fourth and the fifth contours is identical to the direction of the first and the second contours. At first glance, this coincidence seems paradoxical, since the temperature gradient

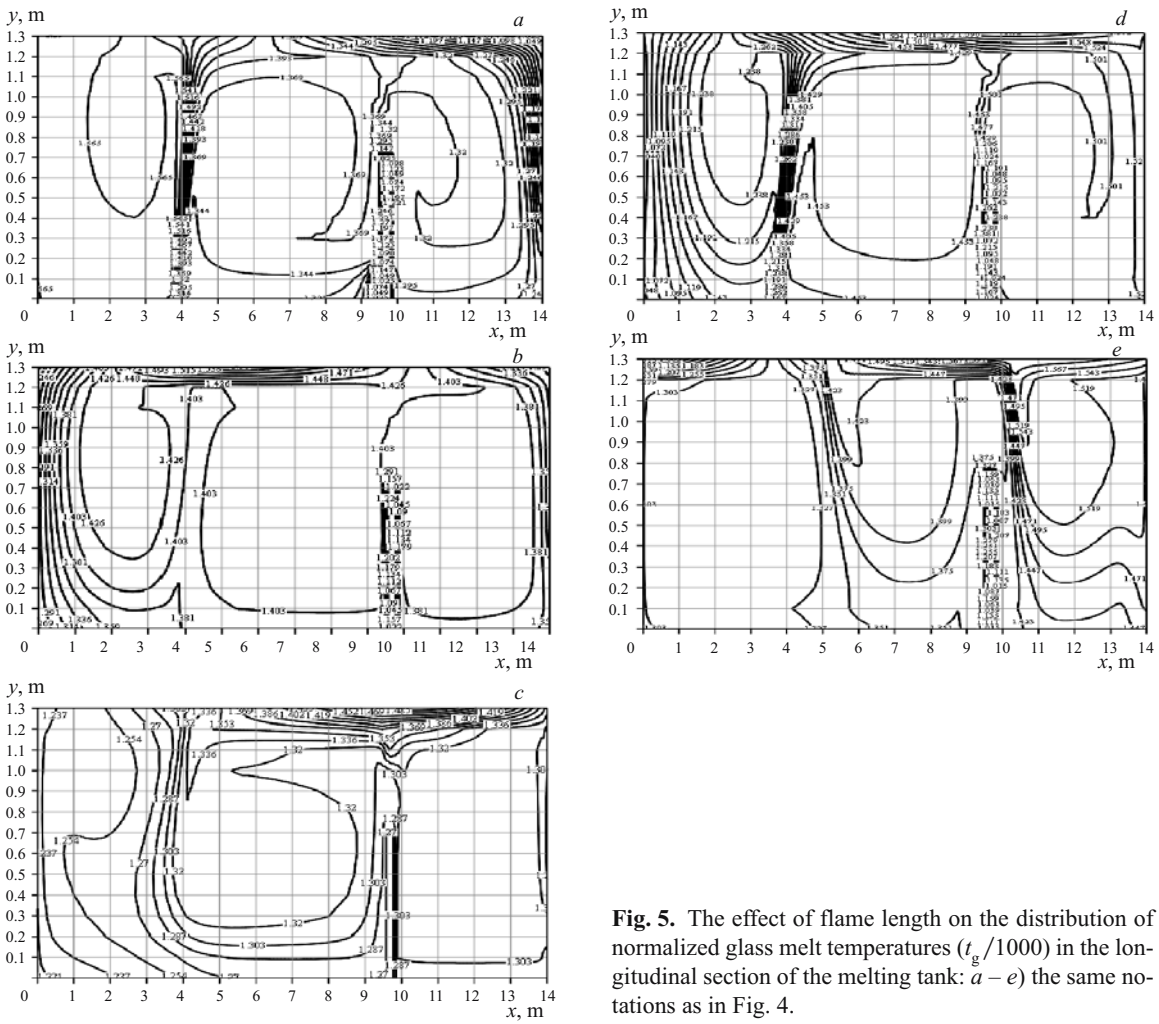

Fig. 5. The effect of flame length on the distribution of normalized glass melt temperatures ($t_g/1000$) in the longitudinal section of the melting tank: *a* – *e*) the same notations as in Fig. 4.

across the glass depth in the planes dividing the contours has different directions. At the same time, it is known a flow of material determined by a nonisothermal medium may be directed either toward decreasing, or toward increasing temperatures. The effect of temperature on convection is not direct and is manifested by means of other factors [4], including the temperature dependence of viscosity and taking working glass from the tank bottom. The latter factor is presumably also responsible for the direction of convection flow circulation (from beneath to above). This direction can be developed as well due to the effect of the uplift force, whose origin is determined by the ratio $\bar{t}_{g.\,s} < \bar{t}_{g.\,b}$.

Thus, under a constant thermal load of the furnace, the concentration of heat generated by the flame within the batch zone results in overheated glass melt surface near the loading hoppers and inadmissible (by technological regulations) cooling of clear melt surface. The overall effect of the combination of factors is related to the formation of several glass melt circulation contours, whose presence contributes to a more uniform temperature distribution across the tank depth before the spillway. At the same time, the higher multiplicity of glass melt circulation in the second, third, and fourth contours leads to the excessive consumption of thermal energy. The accumulation of heat in the circulation contours decreases the temperature potential both of the melt surface and its volume. In general, the considered furnace heating schedule appears technologically unjustified and practically inadvisable.

Extending the flame length to the size of the melting zone ($l_{fl}/L_f = 0.662$) leads to a slight decrease in $\bar{t}_{g.\,s}$ and the temperature maximum shifting toward the neck (Fig. 6*a*, curve *2*). The maximum temperature of 1560°C is registered in the section defined by the longitudinal coordinate $x \approx 5.2 – 5.3$ m; starting from this plane, horizontal temperature gradients ($\Delta\bar{t}_{g.\,s}/\Delta x$) are formed toward the loading zone and the working zone, which are equal to 63.8 and 34.0 K/m, respectively. Compared to the variant of heating the furnace with a short flame ($l_{fl}/L_f = 0.334$), both the distribution and the value of the temperature difference in the longitudinal section of the tank change fundamentally. In the batch-loading zone ($x = 0 – 1.5$ m) the temperature of the bottom layer is now higher than the glass surface tempera-

ture. The reverse correlation of these temperatures ($\bar{t}_{g.\,s} > \bar{t}_{g.\,b}$) is observed in the tank sector limited by coordinates 1.5 m < x < 10.4 m. Beyond the spillway the temperature difference is again characterized by the ratio $\bar{t}_{g.\,s} < \bar{t}_{g.\,b}$. The maximum difference between the temperatures of the surface and the bottom melt layer (approximately 155°C) coincides with the coordinate $\bar{t}_{g.\,s}$ (Fig. 6*b*, curve *2*), moreover, the presence of the spillway has virtually no effect on the relation between the values $\bar{t}_{g.\,s}$ and $\bar{t}_{g.\,b}$.

The change in temperature distribution on the surface and across the melt depth related to the increased flame length has a perceptible effect on the tank hydrodynamics. Two circulation contours are formed in the left part of the tank (before the spillway) (Fig. 4*b*). The quellpunkt position corresponds to $x \approx 6.0 - 6.5$ m, which exceeds the longitudinal coordinate of the temperature maximum ($\bar{t}_{g.\,s}$). The possibility of such discrepancy is discussed in [5]. The boundary dividing the contours, the circulation direction, and the $\bar{t}_{g.\,s} > \bar{t}_{g.\,b}$ relation at the coordinate $x \approx 6.0 - 6.5$ m suggest that the formation of convection flows is due to the presence of horizontal temperature gradients on the melt surface. Consequently, the formation of convection flows is caused by the presence of horizontal hydromechanical pressure gradients and not by the uplift force. This conclusion fully agrees with the concept of A. A. Sokolov on the origin of convection glass melt flows [4].

The formation of a single circulation contour in the batch zone stabilizes the glass melt convection flow in the charging cycle. The left bound of this contour is the end wall of the tank (*AH*), whereas the right-hand bound coincides with the extent of the intense combustion zone: $l_i = 0.0662L_f/1.43 =$ 6.3 m. Note the position and the modified coordinates of the convection flow center (Fig. 4). The horizontal coordinate of this center is within the length of the sector where the melt arrives at the tank (*HI*) and with an increasing flame length, it shifts insignificantly toward the working zone. As the surface temperature of this part of the tank decreases, the vertical coordinate shifts insignificantly toward the tank bottom. In general, there is a sufficiently clear dependence of the position of the center of the charging cycle contour on the site where new melt portions penetrate into the glass melt. The formation of convection glass melt flows beyond the spillway is identical to the first variant of fuel combustion ($l_{fl}/L_f = 0.334$).

The comparison of glass melt flows (Fig. 4*a* and *b*) shows that the change in the temperature field on the melt surface caused by the increased flame length reduces the number of circulation contours from five to four. At the same time, a clearly expressed contour of the charging cycle is formed, which is characterized by a high multiplicity of circulation. Its extension along the tank decreases the length of the working cycle contour, whose extent is limited by the presence of the spillway. The higher temperature of the clear glass surface (1283 – 1350°C) than in the variant $l_{fl}/L_f = 0.334$ decreases the temperature difference across the tank depth.

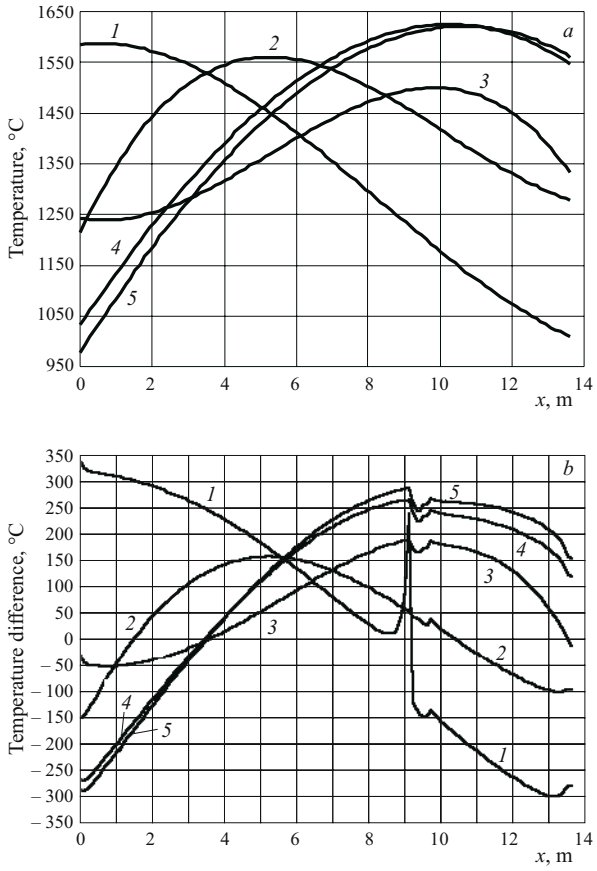

Fig. 6. The effect of flame length on the variation of the average temperature across the width of the working side of the furnace (*a*) and on the distribution of the difference between surface and bottom glass melt temperatures along the tank (*b*): *1 – 5*) $l_{fl}/L_f = 0.334$, 0.662, 1.000, 1.216, and 1.430, respectively.

This fact together with a decreased circulation multiplicity beyond the spillway can account for the melt temperature in the tank neck growing to 1385.5°C.

The temperature field of the glass melt is formed in accordance with the circulation contours (Fig. 5*b*). The position of the isotherms is virtually identical to the shape of the circulation contours. The melt temperature in the contour adjacent to the left wall of the tank is generally heterogeneous. The difference between temperatures of certain areas reaches 220°C. The volumetric temperature distribution is more uniform in the contour adjacent to the left wall of the spillway. The difference between particular glass melt temperatures in the bulk volume is not more than 30°C. A slightly higher (about 35°C) temperature heterogeneity is registered in the area to the right of the spillway. Note also that as the circulation contour transports glass melt from the quellpunkt to the left wall of the tank, the glass temperature in the bottom part of this sector is relatively high and varies from 1376 to 1410°C.

Of special interest is the analysis of modeling tank hydrodynamics for the variant of furnace heating with the full

flame length ($l_{fl}/L_f = 1.0$) and the extent of the intense combustion zone $l_i = 0.7L_f = 9.534$ m. The increased flame length perceptibly modifies the temperature of the glass melt surface (Fig. 6*a*, curve *3*). Compared to the previous variant, $\bar{t}_{g.s}$ is 58.4°C lower. At the same time, the longitudinal coordinate of the maximum $\bar{t}_{g.s} = 1501.6$°C shifts toward the tank neck and corresponds to $x = 10.0$ m, which is 0.4 m further than the coordinate of the right surface of the spillway (*CG*). The temperature gradient arising at the coordinate of the maximum toward the charging site decreases by more than half and the gradient toward the working zone increases: they are equal to 26.5 and 47.4 K/m, respectively.

Substantial changes are registered as well in temperature distribution in the longitudinal section of the tank (Fig. 5*c* and Fig. 6*b*, curve *3*). The considered heating variant has a more uniform temperature field, both before and after the spillway. Only in the batch zone ($x \approx 0 - 3.5$ m) the temperature of the bottom layer exceeds the surface temperature. The maximum temperature difference in this case is not more than 60°C. In the rest of the tank $\bar{t}_{g.s} > \bar{t}_{g.b}$. The maximum difference $\bar{t}_{g.s} - \bar{t}_{g.b} \approx 175$°C, similarly to the previous variant, corresponds to the length of the intense combustion zone. A slightly decreased temperature difference (about 30°C) is observed above the spillway.

The specified regularities of temperature distribution in the tank to a great extent are determined by its hydrodynamics. The shift in the maximum melt temperature $\bar{t}_{g.s}$ toward the neck decreases the number of circulation contours. In the melting part of the tank (batch zone and foam zone) two contours persist, divided along the coordinate $x \approx 8.0 - 8.4$ m. At the same time, their total extent does not go beyond the spillway bounds. A single contour is formed in the clear glass zone, which occupies the entire tank volume after the spillway. The circulation direction of the convection flows in the melting zone, despite the discrepancy between the contour center and the coordinate $\bar{t}_{g.s}$, indicates that the convection flows are due to the existence of a surface area with oppositely directed temperature gradients.

One should note the transformation of the size of the charging cycle contour. Compared to the previous heating variant, the location of the nucleus of the contour remains virtually unchanged. The extension of its longitudinal size occurs due to the horizontal compression of the working cycle contour. The increased size of the charging convection cycle is accompanied by its significantly decreased circulation multiplicity. Despite this fact, the considered variant has the maximum homogeneity of temperature distribution in the glass volume.

The change in the size of the working flow is worth noting. Its geometrical shape and position in the vertical plane are more typical of a local contour than of an extended convection flow. The presence of the spillway not only impedes horizontal extending of the flow, but causes its separation from the tank bottom. The size of the contour in the vertical plane is not more than 3/4 tank depth. The above specifics of hydrodynamics of the melting zone corroborate the need of a detailed investigation of the effect of the spillway height and its location along the tank bottom on the formation of glass melt convection flows.

The leveling of the temperatures of the surface and bottom layers after the spillway (Fig. 6*b*, curve *3*) exclude the uplift force effect on the formation of convection flows. Considering that the longitudinal coordinate $\bar{t}_{g.s}$ virtually coincides with the right plane of the spillway, it appears that the second and third circulation contours should be divided along the surface *CG*. The data in Fig. 4*c* corroborate this conclusion. At the same time, the counterclockwise circulation of the third contour cannot be accounted for by the horizontal temperature gradient on the glass surface. Apparently, the melt convection after the spillway is determined by working glass from the tank bottom. Another distinctive feature of this variant of furnace heating is the high intensity of glass melt circulation after the spillway, which facilitates substantial leveling of temperatures in this part of the tank. The difference between the temperatures of particular sites of glass melt does not exceed 17 – 30°C (Fig. 5*c*), whereas the mean temperature of the melt in the neck is 1353.4°C.

The heating variants with the flame length exceeding the furnace length ($l_{fl}/L_f = 1.216$ and 1.430) preserve the above described regularities of the melt flow. The number of circulation contours and their circulation direction are identical to the variant $l_{fl}/L_f = 1.0$. At the same time, the size of the contours and the numerical parameters of circulation undergo substantial modifications (Fig. 4*d* and *e*). This is due to the effect of the flame length on temperature distribution on the melt surface (Fig. 6*a*, curves *4* and *5*) and in the melt volume (Fig. 5*d* and *e*). Note primarily the change in the maximum temperature value $\bar{t}_{g.s}$, and its longitudinal coordinate x. The flame length equal to $1.216L_f$ and $1.430L_f$ corresponds to $\bar{t}_{g.s} = 1625$ and 1620°C. The former value of l_{fl} at the coordinate $x = 9.9 - 10.0$ m corresponds to horizontal temperature gradients directed toward the charging and working zones: 57.5 and 19.3 K/m, respectively; for the latter temperature value ($x = 10.5$ m) the gradients are 60.0 and 16.0 K/m, respectively. Thus, the extended flame length ($l_{fl}/L_f > 1.0$) increases the gradient of $\bar{t}_{g.s}$ toward the charging zone and decreases the gradient values toward the working zone.

Increasing the length of intense combustion zone up to $l_i = 1.216L_f/1.43 = 11.58$ m fundamentally modifies the relation between the surface and bottom layer temperatures $\bar{t}_{g.s} - \bar{t}_{g.b}$ (Fig. 6*a*, curve *4*). The maximum temperature difference is observed in the batch zone, where $\bar{t}_{g.s} < \bar{t}_{g.b} = 275$°C. Starting with coordinate $x > 3.5$ m, the ratio of temperatures changes for opposite. Before the spillway and the neck it is equal to $\bar{t}_{g.s} > \bar{t}_{g.b} = 270$ and 125°C, respectively. A further increase in l_i ($1.43L_f/1.43 = 13.62$ m) has an insignificant effect on the quantitative parameters and does not qualitatively change the temperature distribution (Fig. 6*b*, curve *5*).

The increase in the horizontal temperature gradient toward the charging zone does not increase the multiplicity of the charging cycle circulation. This is due to a lower glass melt temperature in the batch zone (1000 – 1200°C) compared to the variant with $l_{fl}/L_f = 1.0$. The increased viscosity of the melt, which in certain surface areas reaches 1849.35 Pa · sec, decreases the circulation intensity. In the right-hand part of the tank (after the spillway) a reverse situation is observed. The high temperature of the glass melt surface (1550 – 1625°C) decreases the melt viscosity and intensifies its mixing. In this case the mean temperature of melt in the tank neck perceptibly grows. For the relative flame length $l_{fl}/L_f = 1.216$ and 1.430 it is equal to 1446.8 and 1429.4°C, respectively.

In general, the above considered variants of furnace heating cannot be regarded as technologically advisable. This conclusion is based not only on the low temperature of glass melt surface in the site of batch loading, but also on inadmissibly high temperatures on clear glass surface and at the entrance to the neck.

Based on the results of the calculation of temperature difference across the tank depth (Fig. 6*b*, curves *4* and *5*) it can be assumed that, in accordance with thermogravitation convection criteria, another circulation contour is formed in the tank sector limited by $x \approx 0 – 3$ m. This assumption is based on the fact that similar circulation contours are formed in front of the neck (Fig. 4*a* and *b*) where the condition $\bar{t}_{g.\,s} < \bar{t}_{g.\,b}$ is satisfied as well and contour formation can be determined by the uplift force. However, the data in Fig. 4 (variants *d* and *e*) contradict this hypothesis. In front of the spillway a single convection flow is formed descending along the plane *AH* (Fig. 1). The direction of this flow is determined not only by the horizontal temperature gradient on the melt surface, but also by the temperature dependence of glass density.

Thus, the hydrodynamics of a melting tank on a modern highly efficient furnace depends on a set of interrelated factors. Beside temperature distribution on the glass melt surface determined by exterior heat exchange, convection flows significantly depend on the tank design, batch loading and the glass melt transfer conditions, as well as working flow parameters depending on the specific output of the furnace. The combined analysis of the results of modeling exterior heat exchange [3] and the tank hydrodynamics suggests that with respect to the given furnace design, the most suitable is the heating regime where the total flame length is equal to the furnace length. The length of the intense condition zone (visible part of the flame) in this case is equal to $0.7L_f$.

REFERENCES

1. V. Ya. Dzyuzer and V. S. Shvydkii, “Mathematical model of a glass-melting furnace with horseshoe-shaped flame direction,” *Steklo Keram.*, No. 10, 8 – 12 (2004).
2. V. Ya. Dzyuzer and V. S. Shvydkii, “Mathematical model of hydrodynamics of the melting tank of a glass-melting furnace,” *Steklo Keram.*, No. 1, 3 – 8 (2005).
3. V. Ya. Dzyuzer and V. S. Shvydkii, “The effect of flame length on exterior heat exchange in a glass-melting furnace with horseshoe-shaped flame,” *Steklo Keram.*, No. 7, 3 – 7 (2005).
4. A. A. Sokolov, “Free thermal convection not depending on uplift force,” *Steklo Keram.*, No. 4, 11 – 13 (1984).
5. N. A. Pankova, “The phenomenon of glass melt flowing over the quellpunkt in glass-melting furnaces,” *Steklo Keram.*, No. 9, 14 – 17 (2003).